

Development of a Six-Degree-of-Freedom (6-DOF) Motion Replication Based Production Acceptance Test (PAT)

Michael T. Hale
Dynamic Test Branch
Redstone Technical Test Center
US Army Developmental Test Cmd
(256) 876-0148

Charles W. Freeman II
Dynamic Test Branch
Redstone Technical Test Center
US Army Developmental Test Cmd
(256) 313-1220

Performing quality, Six-Degree-of-Freedom (6-DOF) motion replication testing in the laboratory is rapidly becoming a feasible and attractive alternative to classical 1-DOF methods. This paper considers several of the open issues associated with performing laboratory based 6-DOF vibration testing. A recent 6-DOF laboratory test developed and performed at Redstone Technical Test Center (RTTC) will be used to illustrate the methods employed to aid the test engineer in proper transducer placement, test conduct, and development of the analysis tools used for test documentation purposes.

INTRODUCTION

In the early 1980's, as an alternative to conducting a road test based, Production Acceptance Test (PAT) program for TOW missiles, RTTC developed a novel 3-DOF laboratory based motion replication test [1]. This new test alternative provided a unique methodology which no longer required the use of a M113 and a driver. It also eliminated vehicular and driver risk associated with transporting untested live missiles. The test configuration consisted of three independently controlled servo-hydraulic exciters with associated bearings and spherical couplings, an aluminum fixture, and a tactical M113 missile rack as shown in Figure 1. The three point interface between the exciters and the test fixture allowed motion in the vertical, pitch, and roll mechanical degrees-of-freedom. The control system employed during this test necessitated a significant amount of user intervention, especially when computing the transfer functions required in determining cross-axis effects and when developing subsequent drive files.

Although the 3-DOF system was somewhat cumbersome, it performed reliably for nearly 20 years until it was decommissioned in 2003 as TOW production was perceived to be complete. However, with the onset of the conflict in Iraq, a number of TOW missile variants were introduced and PAT requirements resurfaced. Rather than rebuild the original 3-DOF test assembly, RTTC engineers elected to convert the test to a 6-DOF configuration using a TEAM Model 3 Cube excitation system as depicted in Figure 2 [4]. Control of the 6-DOF motion replication system was demonstrated using both LMS/VXI and Signal Star/SCXI control systems. Given the lack of formal guidance in performing and documenting 6-DOF motion replication testing, it is the intent of this paper to synopsise the current methods employed by RTTC, to use said methods as a precedent for formal guidance, and as advancement in state-of-the-art 6-DOF motion replication technology.

CONVERSION TO 6-DOF

The integration of 6-DOF vibration testing into dynamic test laboratories is entwined with many obstacles requiring an increased level of technical skill from the test engineers planning such tests and from the operators that will ultimately perform the tests. The first step in performing a 6-DOF vibration test in the laboratory begins with acquiring sufficient reference data. In addition to the standard concerns related to the dynamic range and frequency response characteristics of the transducers and recording equipment used in the field data acquisition phase, the quantity and spatial locations of the transducers become critical test parameters. Understanding the underlying dynamics of 6-DOF systems and the physical constraints such systems place on the spatial locations of reference transducers in order to perform true 6-DOF laboratory motion replication is not trivial. Similarly, it is essential that the test operator is able to understand the dynamics of an arbitrary data set that may be provided by an outside source for use as reference data in a laboratory test [2].

It has been shown that the minimum number of acceleration measurements, i.e., the number of reference transducers, needed to estimate angular rate, angular acceleration and linear acceleration is nine [2], [3]. It is has been the experience of this Test Center that performing 6-DOF motion replication tests based on feedback from clusters of three appropriately placed tri-axial transducers significantly improves and simplifies the laboratory test development. Although the use of tri-



Figure 1. 3-DOF TOW/M113 Test Configuration



axial accelerometers

Figure 2. 6-DOF TOW/M113 Test Configuration

introduces an over-determined feedback in the case of a six-exciter 6-DOF platform, it conveniently addresses two problems that are almost guaranteed to surface. First, there will be a difference in mechanical impedance between the field and laboratory which may result in one of the reference transducers aligning closely with a spectral node which will lead to matrix inversion issues during computation of the transfer function. Second, due to the geometry of the unit under test (UUT) and its mounted configuration in the carrier vehicle, planar transducer placement may be the only practical instrumentation option. The basic mathematics describing linear tri-axial transducer placement requirements for 6-DOF laboratory motion replication testing that were used as a basis for the simulation described in this document are found in reference [2]. The following section is an excerpt from reference [2] which revisits the linear transducer placement discussion.

Kinematic Considerations for Transducer Placement

Consider a rigid body equipped with m tri-axial transducers located as shown in Figure 3. The acceleration measured by the i^{th} transducer is given kinematically by:

$$\underline{a}_i = \underline{a}_c + \underline{\dot{\omega}} \times \underline{r}_i + \underline{\omega} \times (\underline{\omega} \times \underline{r}_i), \quad (1)$$

where $\underline{\omega}$ and $\underline{\dot{\omega}}$ represent the angular velocity and angular acceleration of the rigid body and \underline{a}_c represents the acceleration of some reference point on the body and represents the position vector from the reference point to the i^{th} transducer. In general, \underline{a}_c is unknown (unless a transducer was selected *a priori* for that location). Thus, equation (1) represents three vector equations in three vector unknowns (i.e., \underline{a}_c , $\underline{\omega}$, and $\underline{\dot{\omega}}$). True motion reproduction will require knowledge of these three vectors (i.e., 9 parameters) leading to the fact that **at least** three tri-axial transducers (i.e., $m \geq 3$) will be required during the field data collection phase. Additionally, it has been shown that if three transducers are utilized, then they must be distributed such that their relative position vectors are not collinear (i.e., the transducers cannot be placed along a line) [2]. Costello and Jitparphai addressed the three tri-axial transducer measurement method of mapping to an arbitrary point on a body in [3]. Issues associated with the singular nature of the distance matrix which defines the relative position of the measurement points greatly increased the complexity of working with three tri-axial transducer clusters. Addition of a fourth non-coplanar tri-axial measurement point simplifies the time-domain computation greatly and clarifies the importance of the placement of the measurement transducers as addressed by Fitz-Coy and Hale [2]. However, it is important to note that the discussions in [2] and [3] simply justify the use of linear transducers in defining mapping algorithms to define 6-DOF motion at an arbitrary point on a rigid body. In practice, the problem simplifies considerably in that drive files will be generated based on frequency-domain, transfer function based approximations which, in turn, negates time-domain mapping complexities.

Typically, there will be restrictions in the placement of the measurement transducers that may force the transducer placement to approach a collinear configuration. As discussed in [2], this leads to numerical concerns associated with the matrix inversion requirement which is directly related to the positioning of the measurement transducers. A common metric used to study the numerical stability of matrix inversion is the condition number. For this discussion, the condition number, with respect to inversion, is defined as the ratio of the largest to the smallest singular values. A high condition number corresponds to a nearly singular matrix.

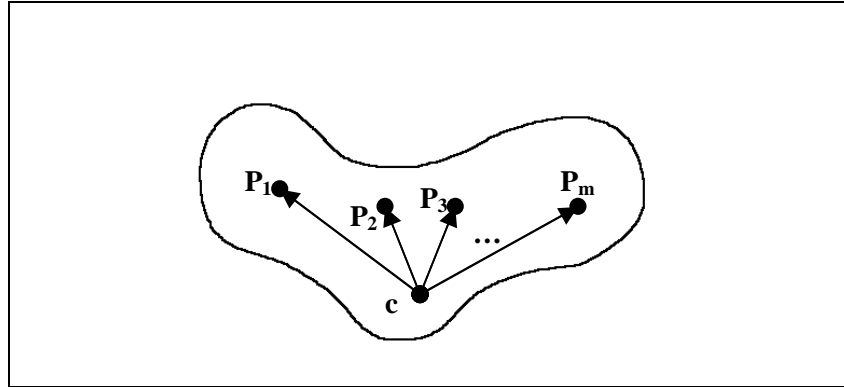


Figure 3. Generic Rigid Body with Transducers

Consider the following example relating to conditioning for a generic $m=3$ case. Three positions are arbitrarily chosen as $\underline{r}_1 = [2 \ 0 \ 0]^T$, $\underline{r}_2 = [1 \ 0 \ 0]^T$, and $\underline{r}_3 = [3 \ 0 \ \varepsilon]^T$ with ε representing the perpendicular distance from the line (x-axis). The relative position vectors and the resulting inertia dyadic are as follows:

$$\underline{r}_{21} = [-1, 0, 0]^T, \quad \underline{r}_{31} = [1, 0, \varepsilon]^T \quad \text{and} \quad \left[\underline{\mathcal{G}}_{\underline{r}_{21}} + \underline{\mathcal{G}}_{\underline{r}_{31}} \right] = \begin{bmatrix} \varepsilon & 0 & -\varepsilon \\ 0 & 2 + \varepsilon^2 & 0 \\ -\varepsilon & 0 & 2 \end{bmatrix}$$

Figure 4 shows the effects of moving the third location away from the x-axis. As ε is increased, the condition number is drastically reduced from infinity to approximately 8 before increasing again. This is expected since as ε increases, the plane formed by \underline{r}_1 , \underline{r}_2 , and \underline{r}_3 once again approaches a straight line (i.e., points 1 and 2 are closely spaced relative to point 3).

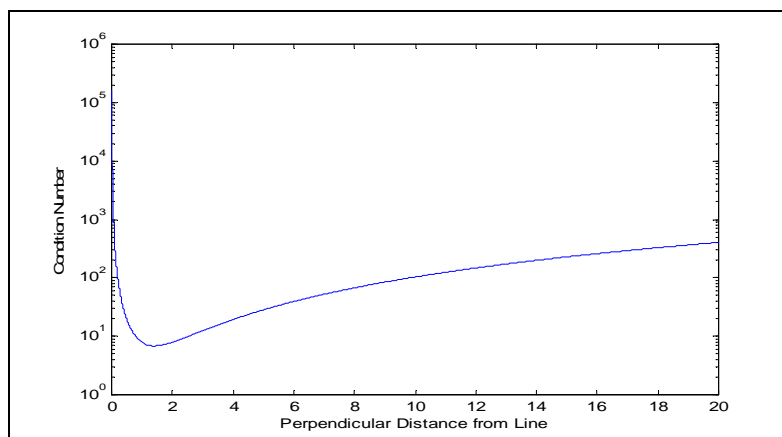


Figure 4. Relative Position Matrix Condition Number as a Function of Perpendicular Distance from a Line Acquisition of Reference Data

LABORATORY TEST

As stated earlier, a TEAM Model 3 Cube, servo-hydraulic excitation system was used to perform the 6-DOF test. In addition to the original PAT requirements, the requirement for testing at temperature extremes (160 °F and -25 °F) was added. The Signal Star/SCXI control system was selected as the control system for this effort. All post-test analysis performed were implemented either via c-script written within the post-processing software framework or via m-files created within the Matlab© environment. The laboratory test consisted of Paved, Gravel, and Cross Country road conditions as summarized in Table 1. Due to the large amount of test data involved, the illustrations provided in the following sections were limited to the Gravel Road scenario. Additionally, also due to the large volume of data, figures illustrating the various analysis techniques are typically limited to one transducer location or a single DOF. If viewing in color, the reference data is shown in blue, laboratory data is shown in red and test tolerances are shown in green.

Table 1. Production Acceptance Road Test Requirements

| Road Condition | Distance (miles) | Average Speed (mph) | Percent of Total Miles |
|-------------------|------------------|---------------------|------------------------|
| Paved | 100 | 25.0 | 20 |
| Unimproved Gravel | 225 | 18.6 | 45 |
| Cross Country | 175 | 12.4 | 35 |

Fixturing and Transducer Placement

For the UUT being considered in this discussion, implementation of the tactically stowed rack was a test requirement. In addition, there was concern with simply mounting the fixture and the rack to the top surface of the cube due to the potential for large rotational moments associated with the separation in distance between the exciter centerline and payload center of gravity. To reduce this concern, the fixture was designed such that the side of the cube served as the mounting point for the lower portion of the rack as shown in Figure 2. The fixture/rack configuration also allowed the transducer placement to have the identical spatial geometry as that of the road test. To address issues with testing at temperature extremes, a thermal barrier was added to the top and side surface of the cube to reduce the heat sink effects of the cube such that minimal thermal effects were encountered by the individual exciters.

Based on the previous discussion from the ‘Kinematic Considerations for Transducer Placement’ section of this paper, three linear tri-axial transducers were placed in a non-collinear manner as shown in Figure 5. Great care was taken to establish a central point to which all measurement locations could be referenced. Measurements and polarity of each transducer were carefully measured and recorded. This process required forethought as to how the UUT will be fixtured in the laboratory to ensure the exact locations may be reproduced in the laboratory. Note from Figure 5 that the positions of the measurement transducers are located at the forward and aft wall and the center floor.

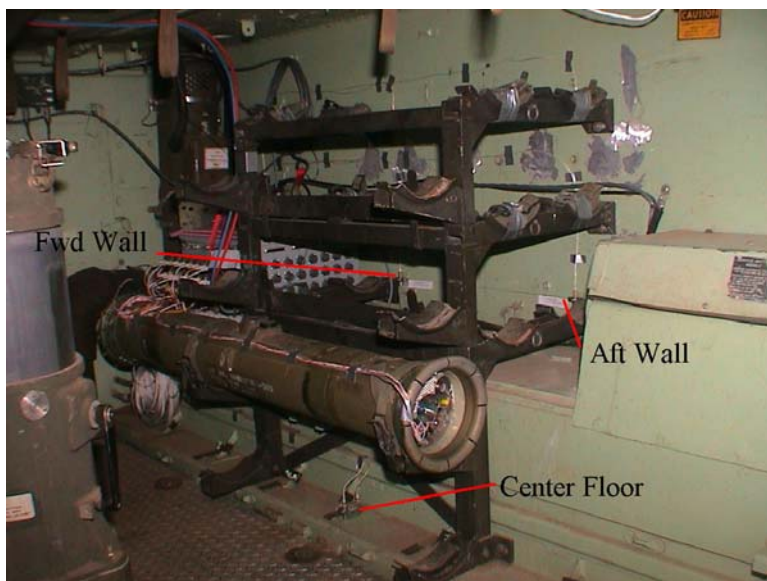


Figure 5. TOW/M113 Missile Rack and Accelerometer Locations

The geometry of this particular UUT was such that meeting the non-collinear measurement requirement was trivial. In addition to the cluster of three tri-axial transducers which will serve as the reference data in the laboratory based motion replication, an instrumented missile was also employed during the actual road testing. This missile was instrumented with tri-axial accelerometers at the forward, mid, and aft sections inside the launch tube. Placing the instrumented missile in the exact same location and orientation during the laboratory test allows a point-to-point comparison between the response data and the field data. This comparison provides an additional metric for consideration in evaluating the laboratory simulation.

The PAT requirement consisted of a 500 mile road test as distributed in Table 1. A further subdivision of speed distribution was performed by applying a Beta distribution [1]. Using the distribution of speed as a guideline, a 15 minute mission was planned in which the reference data would be acquired. Due to limitations in road course lengths, the test driver was required to turn around and repeat the course. Recording equipment remained on during the entire process and the turn around events were extracted during development of the reference files ultimately used in the laboratory test.

Development of Reference Files

The field data used to develop the reference files utilized during this motion replication test was acquired from a M113 equipped with a MARS data recorder which was subsequently dubbed to a Metrum RSR-512 digital tape recorder. A National Instruments PCI-6071E data acquisition card was used to digitize the dubbed data into standard ASCII format. Once resident on the analysis computer, all data channels were imported into Matlab and a pre-test data review was initiated.

Regarding the pre-test data review, it is essential to overall test validity and efficiency since placement and orientation of transducers are paramount to motion replication simulations. Misalignment of one transducer will adversely affect the transfer function matrix as a whole. Great care should be taken to ensure these types of problems do not occur since they will affect not only the vibrational aspects of the test but to a larger degree, angular motion and phase control concerns. To address these types of issues, several checks were instituted. Detailed measurements and photographs of the actual setup (i.e., how and where the item was mounted) were taken to aid in proper laboratory setup since it should mimic the field setup as accurately as possible. In addition, once the UUT and associated measurement and control instrumentation are configured in the laboratory, phase and coherence measurements between drive channels and control channels were examined to make sure that input points and their resultant responses were logical (e.g., a vertical input should largely affect vertical responses at low frequencies). Also, Power Spectral Density (PSD) plots of the reference and the laboratory data files were analyzed, real-time, at coinciding speed-time intervals to verify frequency response, axis, magnitude, and tonal information relative to each speed.

After the pre-test data review, a MATLAB script was used to construct the reference files based upon a predetermined scenario table. The aforementioned script split the data channel matrix into columns, re-sampled each data channel to a convenient block size, extracted user defined time intervals (to eliminate voiced turn-arounds, dropouts, and unacceptable speed fluctuations), smoothed the endpoints, and concatenated the smoothed intervals into one contiguous data file that encompassed all speeds for that data channel. As a final step, an International Sectoral Data Base (ISDB) header block was added to the top of each newly constructed data file to allow it to be imported into the Signal Star/SCXI motion replication control software. After all the required data files were imported into the controller, they were filtered to 150 Hz and converted to reference curves as necessitated by the control software. The resulting curves were used as the reference for each laboratory simulation. Additionally, prior to performing an actual laboratory simulation, each reference was analyzed at a higher resolution within the control software to ensure data integrity. Knowing that, for a tracked vehicle, the frequency of the primary periodic will occur at approximately three times the vehicle speed, the Fast Fourier Transform (FFT) of each block was analyzed and the corresponding tonal information was used to verify each stated speed. If a discrepancy in the correlation between speed versus primary periodic exceeded ± 5 percent then that block was dropped. Once the block drop procedure was completed, the reference files were divided into control sequences, which represented the required vehicle speeds, and a low level equalization pass was initiated.

The low level passes, typically 6dB and 3dB below actual test levels, calculate an average transfer function over the duration of the simulation. This transfer function is periodically updated during each pass and is continued until sufficient convergence is detected. Once converged, the controller is stepped up to full level and the actual simulation begins. The Signal Star control system enables the transfer function update process to continue during the full level passes eliminating the need to estimate a new transfer function during subsequent passes caused by normal dynamic deviations within the test setup.

Test Alarm and Abort Criteria

One weakness associated with performing motion replication tests for events that are non-stationary, with respect to either spectral or energy content, is the lack of parameters available in current control algorithms that monitor and abort a test in the event of a predetermined divergence criteria. Although it contains no phase information, RMS versus time, calculated as:

$$x_{rms}(i) = \left[\frac{1}{M} \sum_{n=((M^*i)-M)+1}^{M^*i} (x(n)^2) \right]^{\frac{1}{2}}, i = 1, \dots, \text{floor}\left(\frac{N}{M}\right), \quad (2)$$

where, N is the length of record $x(n)$, M is the number of points in the time averaging process, and $\text{floor}(N/M)$ rounds N/M to the integer value nearest minus infinity, serves as a good reference metric in addressing simulation performance. In fact, RMS versus time is one of the few parameters that may be used as test abort parameters in either of the control systems that were considered in this effort. Spectral based tolerances are difficult to employ during a motion replication test since the spectrum is time variant over the duration of the test.

For the original 3-DOF PAT test, an RMS tolerance of ± 20 percent was employed at each of the three control points. For the 6-DOF PAT test being considered in this discussion, an RMS tolerance of ± 25 percent was employed at each of the nine control points. To illustrate the test performance in terms of RMS versus time, the Aft Wall triaxial accelerometer reference data, laboratory data and ± 25 percent tolerance are shown in Figure 6. The linear time constant used in the RMS calculation was 5 seconds.

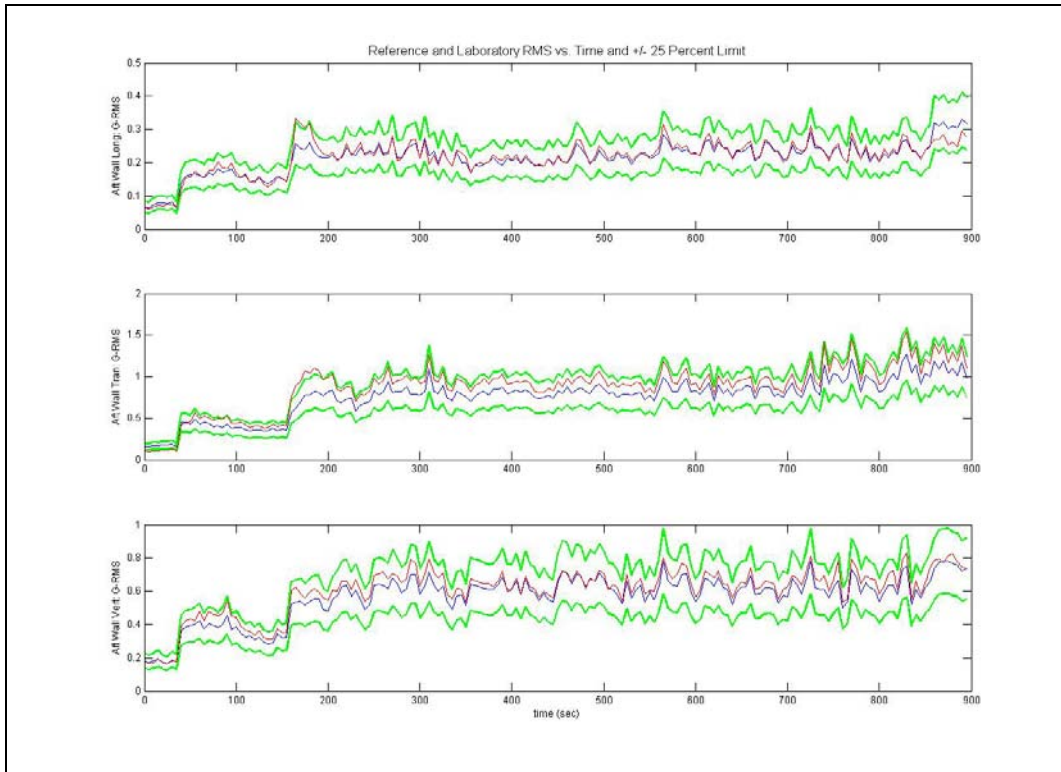


Figure 6. Performance Example - RMS vs. Time

POST TEST ANALYSIS

In addition to the RMS versus time analysis that is performed real time, this section is intended to provide a summary of additional analysis techniques that are generally performed post-test in order to document and provide

an indication of the fidelity of the motion replication test. Note that ideally all of the analysis techniques listed would be performed real time; however, most are not integrated into the current M-DOF control systems. Also observe that the test tolerances discussed in this document are specific to the UUT. Discussion is still open regarding establishing general tolerances for 6-DOF motion replication. Although establishing general guidelines for test tolerances is reasonable, it is strongly recommended that the UUT specific test objectives be considered when establishing test tolerances.

Power Spectral Density

As mentioned in the previous section, even though the spectral properties of the motion replication test discussed in this paper are time variant, an average PSD plot is computed for each of the nine control channels and compared to PSDs computed for each of the nine reference channels. It is recognized that instantaneous spectral content of the the resulting PSD will have been averaged, however, it still serves as another metric in addressing overall system performance. Another spectral based view of the test data in which the spectral smearing is reduced is through use of the Short Time Fourier Transform or even a Wavelet Based analysis.

For this test effort, PSD's actually served as a test metric. For the original 3-DOF test, with the understanding that the reference signal was nonstationary as a result of the speed variations, it was agreed to compute an average PSD of each of the three reference signals. A maximum of the three PSD's plus 3dB was then established as the test tolerance. Recall that the three reference signals were all vertical axis in the original 3-DOF test. For the upgraded 6-DOF test, a similar test tolerance was established for each of the three mutually orthogonal linear degrees-of-freedom. This technique is illustrated below in Figure 7.

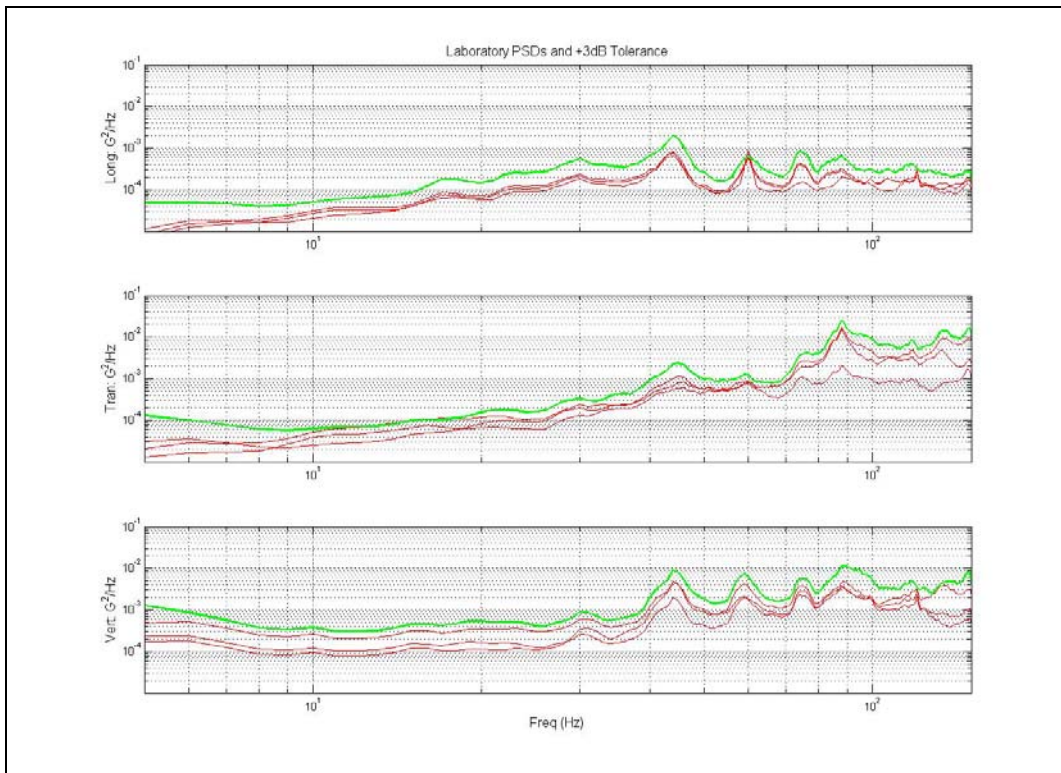


Figure 7. PSD vs. PSD Tolerance for each Linear DOF

Crest Factor

The crest factor provides a quick and convenient measure of the ability of the simulation to maintain similar peak levels as a ratio of the overall RMS level of the reference signal. Crest factor versus time, calculated as:

$$x_{CF}(i) = \frac{\max\{abs[rect(((Mi) - M) + 1, Mi)x(n)]\}}{x_{rms}(i)}, i = 1, \dots, floor\left(\frac{N}{M}\right), \quad (3)$$

where M , N , and $floor(N/M)$ as defined for Equation (2). Using the Aft Wall Transverse as an example, Figure 8 illustrates the laboratory test performance in terms of Crest Factor. To provide a feel for signal magnitude, the corresponding RMS versus time and G-Pk versus time are also included with the Crest Factor plot.

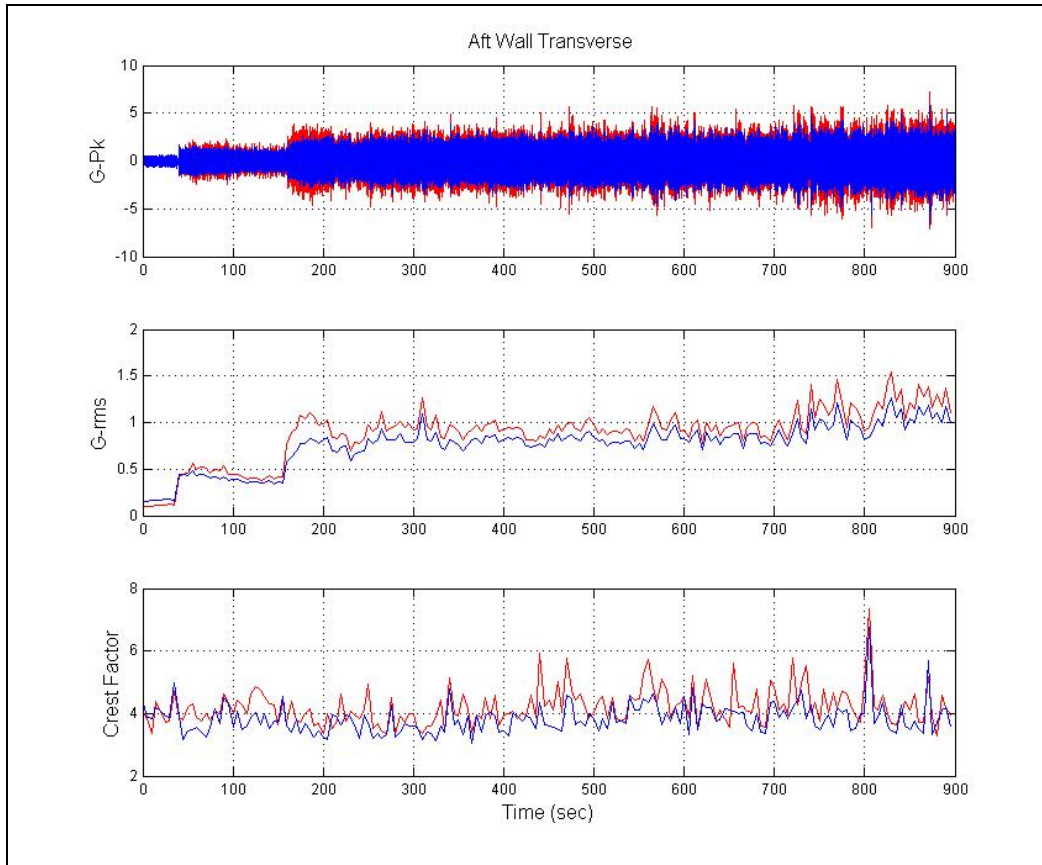


Figure 8. Performance Example – Aft Wall Transverse Crest Factor vs. Time

Transfer Function

The PSD analysis described in the previous paragraph provides a general spectral view of the reference data; however, it contains no phase information. It is the differences in phase and amplitude between collinear accelerometers that indicate angular motion. One method of investigating the presence of angular acceleration from a suite of linear accelerometers is to perform complex transfer functions between collinear pairs of linear accelerometers. Subsequently, performing the same transfer function analysis between the same locations in the laboratory provided another metric for measuring the fidelity of the laboratory test. Analyzing the transfer functions corresponding to the field and laboratory measurements often indicates where the mechanical impedance between field and laboratory begin to diverge. Referring back to the PSD measurements, one is able to gain some perspective as to the amount of energy present as a function of frequency and thereby gain perspective in to the deviations expected as a result of divergence in mechanical impedance. This technique is illustrated in Figure 9 using the Forward and Aft Wall Vertical channels. Note that gain other than unity or phase other than zero radians indicate the presence of Pitch motion. Given the similarities between the reference and laboratory transfer functions, one would expect similarities in the Pitch estimates.

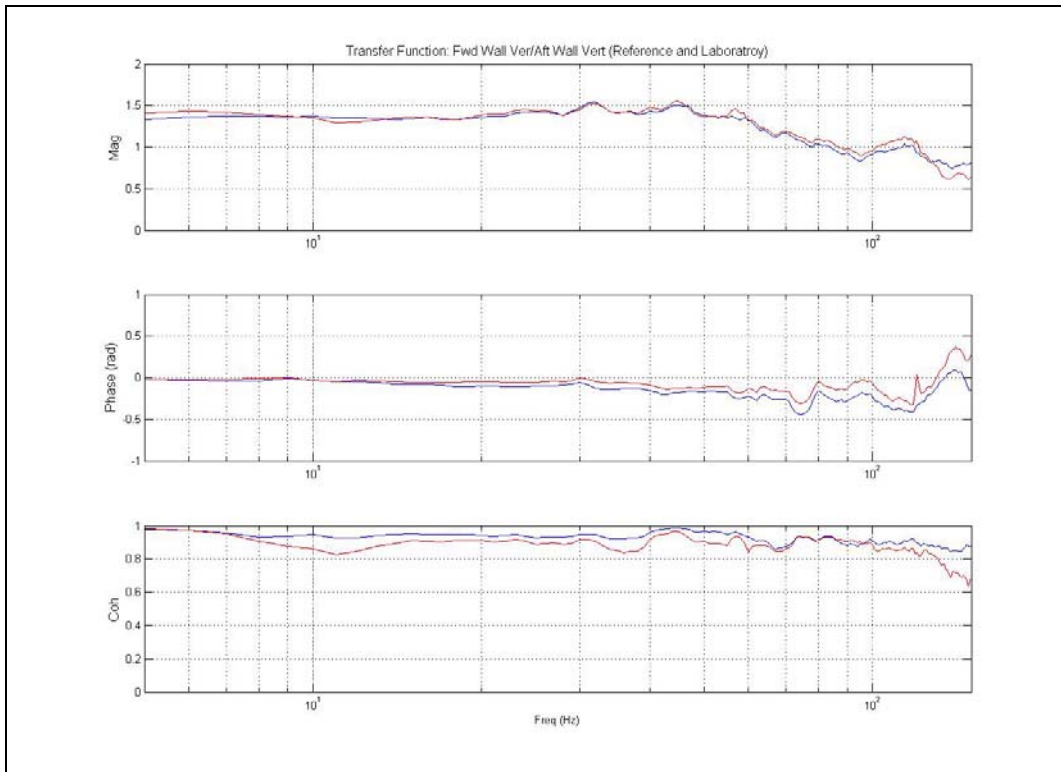


Figure 9. Performance Example - Transfer Function of Fwd Wall/Aft Wall Vertical Indicating the Presence of Pitch Motion

Angular Motion Estimations via Small Angle Approximation

In an effort to address the level of fidelity associated with rotational degrees-of-freedom from a test controlled entirely by feedback obtained from linear accelerometers, small angle approximations of angular motion were developed from both the field data and corresponding laboratory accelerometer pairs and the results were compared. Since the maximum angular motion the 6-DOF exciter being employed is limited to ± 6 degrees, the error associated with the approximation will be negligible. Ideally this technique will provide a good metric for analyzing the angular motion for the rigid body case. The frequency, at which the field data and laboratory data begin to diverge, is an indication of where the mechanical impedance between tactical field mechanical interface and laboratory fixturing begins to differ. The magnitude of the divergence provides some idea of the quality of the impedance match.

To illustrate this concept, Table 2 lists the pairs of accelerometers that were used to develop small angle approximations of angular acceleration for each of the three rotational DOF. Note that pairs of linear accelerometers other than those that correspond to specific examples illustrated within this document, as listed in Table 2, could have been selected to estimate the angular acceleration. It is recognized that the instantaneous center of rotation (ICR) may not coincide exactly with the ICR of the test platform and that the angular motion estimates may in fact be vectors that are not perfectly orthogonal with respect to the true axis of rotation. However, as long as the laboratory reference linear accelerometers used to make the angular acceleration estimates correlate to the exact location and phase of the reference measurements, a localized angular motion comparison is still of interest in addressing replication fidelity.

Although not available for this test, even though it may be band-limited, it is recommended that whenever possible an angular accelerometer be placed at the midpoint between the linear accelerometers being used to estimate a rotational DOF of interest. The addition of the angular accelerometer will provide a direct measure of ground truth of angular acceleration at a particular point on a structure.

Table 2. Accelerometer Placement used to Compute Angular Acceleration Estimates

| Rotational DOF | Accelerometer #1 Location | Accelerometer #2 Location | Distance Between Accelerometers (in) | Angular Acceleration (rad/sec ²) |
|----------------|------------------------------|-------------------------------|--------------------------------------|--|
| Pitch | Fwd Wall Vert (12,18.5,18.5) | Aft Wall Vert (-12,18.5,18.5) | 2l=24 | $\frac{(a_{1z} - a_{2z}) * 386}{2l}$ |
| Roll | Center Floor Tran (0,0,0) | Aft Wall Tran (-12,18.5,18.5) | 2l=28.78 | $\frac{(a_{1z} - a_{2z}) * 386}{2l}$ |
| Yaw | Fwd Wall Tran (12,18.5,18.5) | Aft Wall Tran (-12,18.5,18.5) | 2l=24 | $\frac{(a_{1y} - a_{2y}) * 386}{2l}$ |

Figure 10 illustrates the time domain comparisons between angular motion approximations between the field and the laboratory data. Figure 11 illustrates the frequency domain comparisons in the form of PSD's of the angular motion approximations between the field and the laboratory data. The 3dB test tolerance was based on the reference angular accelerations as estimated per Table 2. Figure 12 illustrated the frequency domain comparisons between the reference and the laboratory comparisons of the Pitch estimates in terms of a transfer function of the estimates. Observe that the magnitude of the Pitch estimate falls within the ± 25 percent guidelines set for this test. However, note the increase in phase correlation as frequency increases. Fortunately, as it was for this test, phase accuracy is generally more important at lower frequencies where displacement is higher; however, one should address this parameter based on the test objectives specific to the UUT.

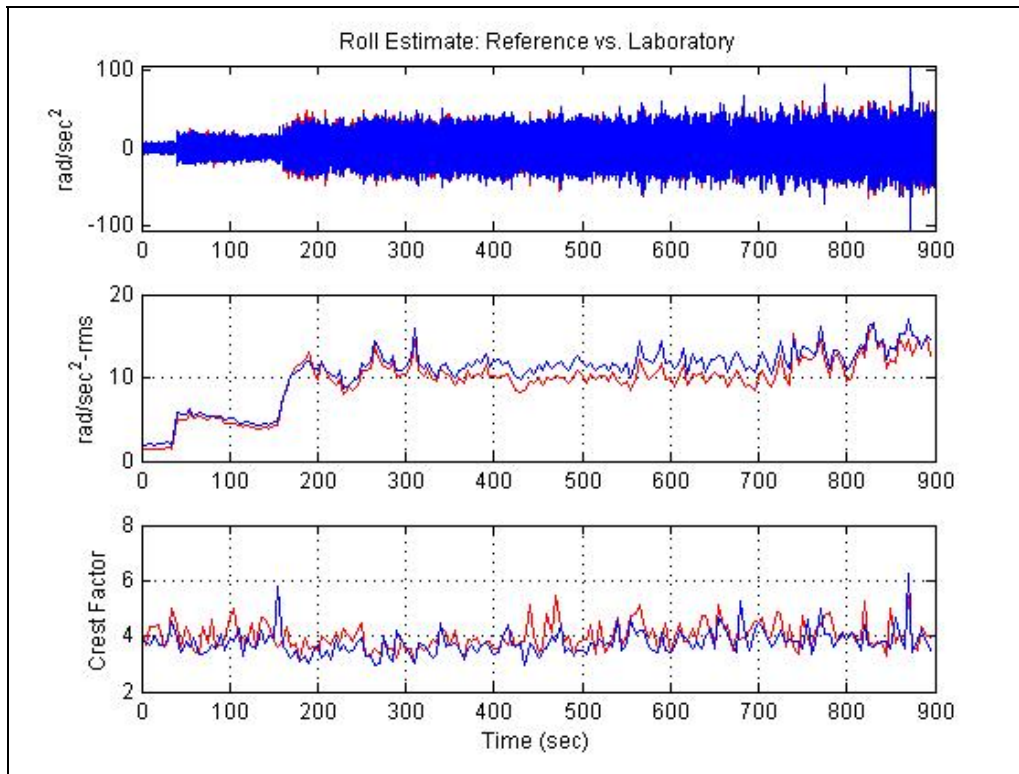


Figure 10. Performance Example – Time Domain View of the Roll Reference vs. Laboratory Estimates

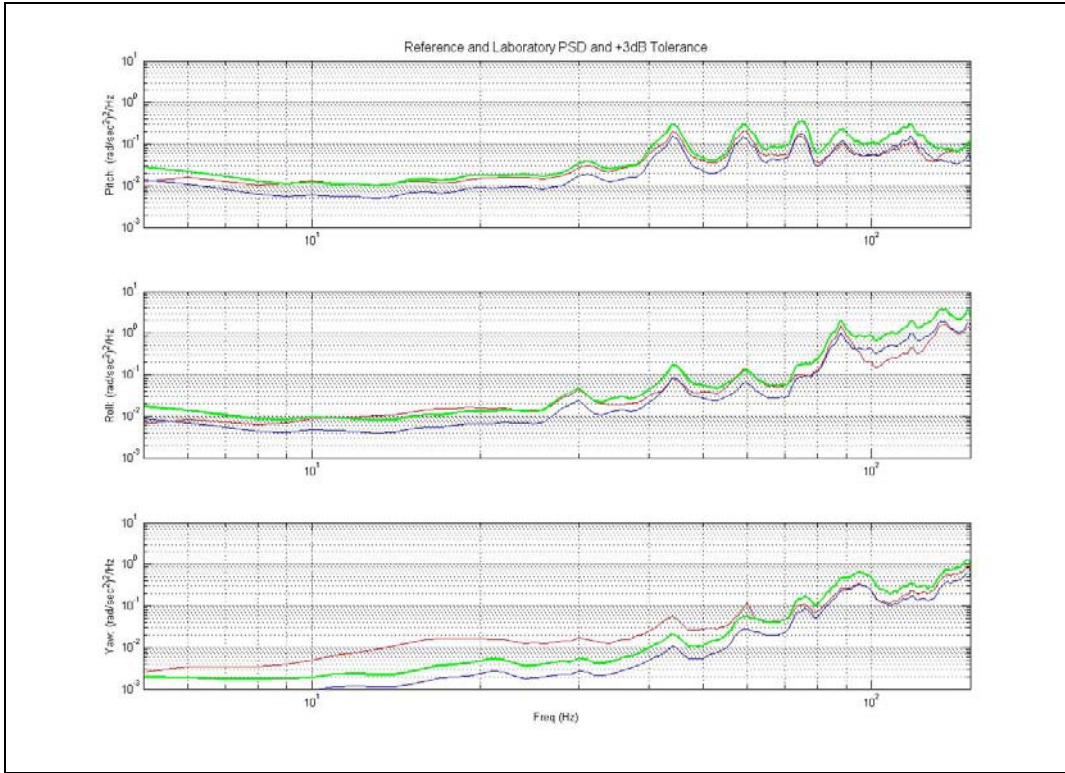


Figure 11. PSD's of the Angular Acceleration Estimates - Reference vs. Laboratory

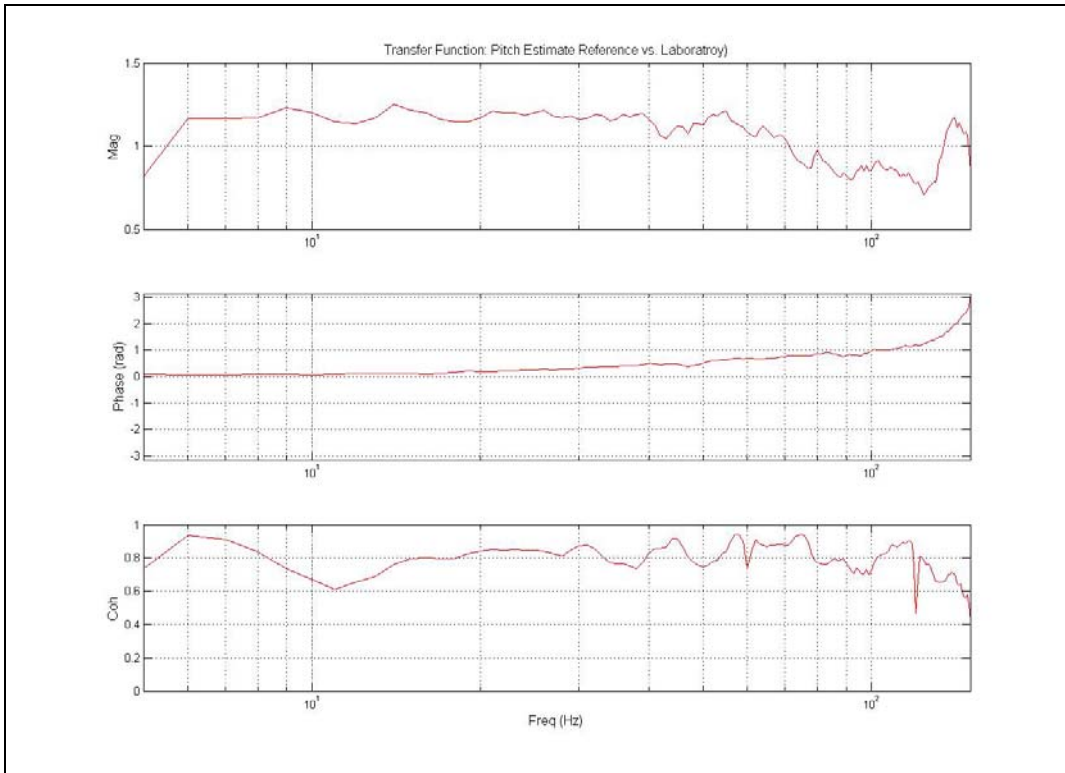


Figure 12. Transfer Function of Pitch Estimates – Reference vs. Laboratory

Probability Density Function

A histogram provides a simple method of graphically summarizing the distribution of a univariate data set. The features of a histogram such as the center, spread, skewness, and presence of outliers provide indications of the distribution model of the data set. In general, the fidelity in which the laboratory simulation is able to replicate non-parametric behavior is a key advantage attained by motion replication system testing as opposed to the normal distribution that would be associated with a traditional 1-DOF vibration control system using a PSD as a reference.

When viewing histograms one may wish to compare the probability distribution function (PDF) of the signal of interest to that of common PDF's such as a Normal PDF or even parametric distribution functions if classic PDF's fail to produce a good curve fit. Figure 13 illustrates the histograms and corresponding Normal PDF curve fits between the Fwd Wall Long axis acceleration associated with the gravel road data set and the fidelity in which the laboratory simulation is able to replicate the characteristics of the probability distribution function.

Observe that the data set of interest is in fact highly Gaussian in structure for this case. In addition to serving as a metric in accessing simulation performance, knowledge of the PDF characteristics enables the user to apply time compression techniques if desired. For example, if the data set has a strong Normal PDF characteristic, Minor's rule may be employed using the same approach as in traditional vibration testing. For other than Normal PDF's, alternate compression techniques exist.

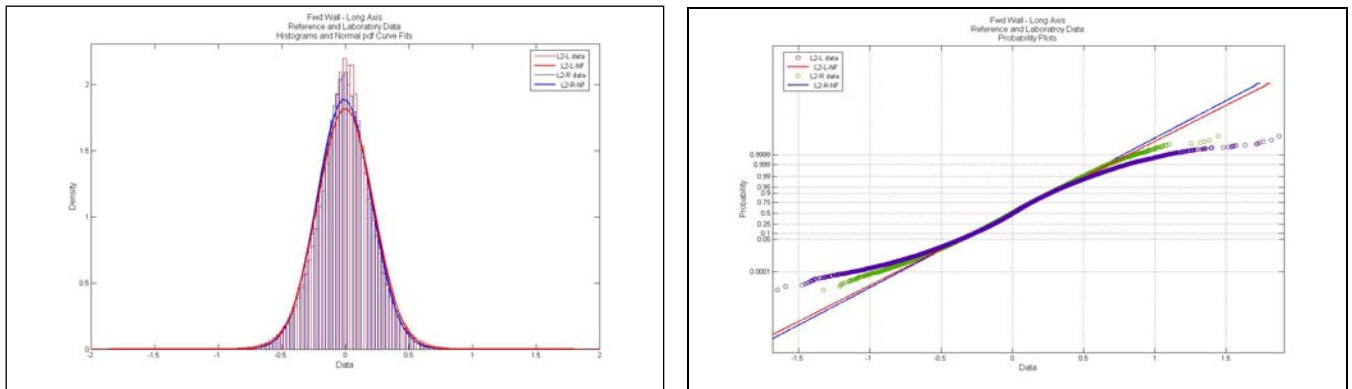


Figure 12. Histogram and Normal Curve Fit and Corresponding Probability Plot of Fwd Wall Long

CONCLUSIONS AND FUTURE WORK

To date, minimal formal guidance for the conduct of 6-DOF vibration tests is provided by the Military Standards, ITOP's, or NATO documents that traditionally serve as guidelines to the industry. It was the intent of this paper to illustrate through an example some of the benefits of 6-DOF testing and to provide metrics for consideration in establishing performance metrics. It was shown that, in addition to the fidelity enhancement associated with the addition of the rotational DOF, 6-DOF motion replication provides a method of performing a non-parametric test.

Currently, the test operators skill and experience remain a key factor in performing a motion replication test. Much of the post test analysis discussed would have been performed prior to the actual test event using surrogate hardware, providing the operator some *a priori* information regarding test performance which may be monitored on an independent analysis system. As experience is gained in this area, it will be relayed to the appropriate vendors and/or working groups addressing 6-DOF testing guidelines.

REFERENCES

- [1] Hale, Michael, TOW Production Acceptance Test Program Test Procedure for M113 Road Test Vibration Simulator, Rev 2, SR-RD-TE-90-67.

- [2] Fitz-Coy, Norman and Hale, Michael, Spatial Requirements for Linear Transducer Measurements and Excitation Point Mapping in Six-Degree-of-Freedom Vibration Testing, Proceedings of the 65th Shock and Vibration Symposium, Nov. 2000.
- [3] Costello, Mark and Thanat, Jitraphai, Determining Angular Velocity and Angular Acceleration of Projectiles Using Tri-axial Acceleration Measurements, Journal of Spacecraft and Rockets, vol 39, Jan – Feb 2002.
- [4] Team Corporation, 11591 Watertank Road, Burlington WA 98233.
- [5] Hughes, Peter, Spacecraft Attitude Dynamics, John Wiley & Sons, 1986.
- [6] Battin, Richard H., An Introduction to the Mathematics and Methods of Astrodynamics, Revised Edition, AIAA Educational Series, pg 345, 1999.